Environmental Earth Sciences (2020) 79:308
https://doi.org/10.1007/s12665-020-09055-7

ORIGINAL ARTICLE

Modeling permafrost distribution over the river basins of Mongolia using remote sensing and analytical approaches

Munkhtsetseg Zorigt[1,2] · Khulan Myagmar[1] · Alexander Orkhonselenge[3] · Eelco van Beek[2,4] · Jaap Kwadijk[2,4] · Jargaltulga Tsogtbayar[5] · Jambaljav Yamkhin[6] · Dorjsuren Dechinlkhundev[7]

Received: 4 October 2019 / Accepted: 8 June 2020 / Published online: 15 June 2020
© Springer-Verlag GmbH Germany, part of Springer Nature 2020

Abstract

The spatial distribution of permafrost and associated mean annual ground temperature (MAGT) and active layer thickness (ALT) are crucial data for hydrological studies. In this paper, we present the current state of knowledge on the spatial distribution of the permafrost properties of 29 river basins in Mongolia. The MAGT and ALT values are estimated by applying TTOP and Kudryavtsev methods. The main input of both methods is the spatially distributed surface temperature. We used the 8-day land surface temperature (LST) data from the day- and night-time Aqua and Terra images of the moderate resolution imaging spectroradiometer (MODIS). The gaps of the MODIS LST data were filled by spatial interpolation. Next, an LST model was developed based on 34 observational borehole data using a panel regression analysis (Baltagi, Econometric analysis of panel data, 3 edn, Wiley, New York, 2005). The model was applied for the whole country and covered the period from August 2012 to August 2013. The results show that the permafrost covers 26.3% of the country. The average MAGT and ALT for the permafrost region is − 1.6 °C and 3.1 m, respectively. The MAGT above -2 °C (warm permafrost) covers approximately 67% of the total permafrost area. The permafrost area and distribution in cold and warm permafrost varies highly over the country, in particular in regions where the river network is highly developed. High surface temperatures associated with climate change would result in changes of permafrost conditions, and, thus, would impact the surface water availability in these regions. The data on permafrost conditions presented in this paper can be used for further research on changes in the hydrological conditions of Mongolia.

Keywords Permafrost distribution · Remote sensing · Panel data · Land surface temperature · Thaw depth

Introduction

Permafrost is found in large parts of Mongolia, predominantly in the Khentii, Khuvsgul, Khangai, and Altai mountains which are the main sources of surface water in the country. The dynamics between surface water and the various types of permafrost is not well understood. Recent studies show that climate change impacts the permafrost in the country. Studies show an increase in mean annual ground temperature along the Khuvsgul and Khentii mountain transect of 0.2 till 0.5 °C in 35 years since the 1980s (Kynický et al. 2009). The highest increase occurred in the Khuvsgul mountain range where the mean annual ground temperature (MAGT) and the active layer thickness (ALT) have increased by, respectively, 0.1–0.3 °C and 5–20 cm (Sharkhuu and Anarmaa 2012). To understand how the surface water system responds to the degrading permafrost, we have to characterize the permafrost properties at basin level. The spatial

✉ Munkhtsetseg Zorigt
z.munkhtsetseg@gmail.com

1 School of Engineering and Applied Sciences, National University of Mongolia, Ulaanbaatar, Mongolia

2 University of Twente, Enschede, The Netherlands

3 Laboratory of Geochemistry and Geomorphology, School of Arts and Sciences, National University of Mongolia, Ulaanbaatar, Mongolia

4 Deltares, Delft, The Netherlands

5 School of Arts and Sciences, National University of Mongolia, Ulaanbaatar, Mongolia

6 Permafrost Sector, Institute of Geography and Geoecology, Mongolian Academy of Sciences, Ulaanbaatar, Mongolia

7 Institute of Fresh Water and Ecosystem, Ulaanbaatar, Mongolia

variability of MAGT and ALT at basin scale is fundamental information for this purpose. Because of lack of observational data, we have to model the spatial distribution of permafrost and its properties MAGT and ALT. Recent studies use modified and reconstructed land surface temperature (LST) of MODIS. The LST data of MODIS are a promising source of input data for spatially distributed and statistical permafrost models (Langer et al. 2013; Wu et al. 2018a, b; Niu et al. 2018), for assessment of thawing and freezing indices (Hachem et al. 2009) and for mapping (Neteler 2010; Langer et al. 2013; Mustrer et al. 2015; Zou et al. 2017). Comparison with observations shows that MODIS LSTs are reliable and consistent under clear sky conditions (Hall et al. 2008). The main problem with satellite data is cloud contamination (Neteler 2010) and other reasons causing spatial and temporal gaps in the datasets. Data with different time intervals of MODIS LSTs have all missing values. Partly, this can be overcome using 8-day LST data (Zou et al. 2017). Application of different approaches for spatial and temporal interpolation to fill the gaps in the data series has been reported in the literature. Harmonic analysis time-series for several regions such as the Tibetan Plateau, the Middle East including Iran, Turkmenistan, and the Caspian Sea were applied by Xu et al. (2013), Zou et al. (2017), and Malamiri et al. (2018). Integrated methods to fill the gaps are also used in the US (Huang et al. 2015; Pede and Mountrakis 2018), based on temporal and spatial interpolation (Metz et al. 2017). All these methods can be considered to be successful depending on the purpose of the research.

In this study, we present the distribution of permafrost and its properties in Mongolia using the MODIS satellite data. The land surface temperatures were modeled using a panel regression analysis which works to intercorporate cross-sectional and time-series data (Baltagi 2005). It is developed in economic sectors, but has been used in studies in geography. Several studies used the panel regression to develop models and analysis as a way of applying remote-sensing data (Yu 2015; Shi et al. 2016; Qi et al. 2017). The panel regression gives possibilities of the different types of analysis based on how panel data were created. To perform this purpose, we tested the hypothesis (1) topographic features are independent factors for the panel regression model. The analysis for the measure surface temperatures from the 34 boreholes and the topographic features (elevation, latitude, longitude, and slope) with four datasets from Aqua/Terra images of the MODIS. Then, TTOP approach and the Kudryavtsev model were used to simulate the MAGT and ALT values. In the context of this paper, cold permafrost is defined when the mean annual ground temperatures are below − 2 °C. These are mainly found in the continuous permafrost zone. Warm permafrost is defined for temperatures above − 2 °C (Smith et al. 2010; Wu et al. 2010). These are found in the discontinuous permafrost zone (Romanovsky et al. 2010). The developed model is capable to calculate the cold and warm permafrost and its properties for the 29 river basins distinguished in Mongolia. Therefore, the further hypothesis (2) developed that cold permafrost is predominated in the river basins underlying by permafrost. The modeled thaw depths and MAGT distribution over the river basins can be a main input for future research on the link between the surface water cycle and the permafrost region in Mongolia.

Materials and methods

Borehole data

Permafrost in Mongolia is distributed as continuous, discontinuous, or sporadic/isolated extent, and is covered about 29.3% of the total territory (Jambaljav et al. 2017). According to maps and publications on distribution of permafrost in Mongolia, it is predominantly occupied in the Khentii, Khuvsgul, Khangai, and Altai Mountain Ranges and their surrounding areas. The development and distribution of the permafrost are mainly dependent upon the continental climate and mountainous terrain (Ishikawa et al. 2018), and characterized by arid region and mountain permafrost (Zhao et al. 2010). Region of the permafrost in the country is formed as the Southern limit of the Siberian permafrost and its temperatures are close to 0 °C, and thus, they are thermally unstable (Sharkhuu 2003).

In this study, we have used 34 permafrost observational sites in Mongolia with data covering the period August 2012–August 2013 collected by Permafrost sector in Institute of Geography of Mongolia. These boreholes are found in the Altai, Khuvsgul. Khangai and Khentii mountain range where permafrost occurs (Fig. 1). The elevation of the boreholes varies from 1405 to 2695 m a.s.l. From the overall 34 boreholes for the study, 7 boreholes in the Khuvsgul mountain range, 11 boreholes in the Khangai mountain range, 3 boreholes in the Khentii mountain range, and 13 boreholes in the Altai mountain range (data of ground temperatures and soil characteristics of the 34 boreholes used to the study; Table 1).

The boreholes were installed with HOBO U12-4 loggers to measure the ground temperatures in 4-h time intervals. The boreholes were drilled from land surface to 15-m deep and ground temperatures were measured occasionally (Table 1). From these measurements, we calculated MAGT which is temperature of the base of active layer. The base of the active layer occurs at a place where the maximum ground temperature equals to 0 °C and a linear interpolation is carried out. Then, MAGT is determined by interpolation of averaged ground temperatures from the measurements. The borehole measurements indicated that

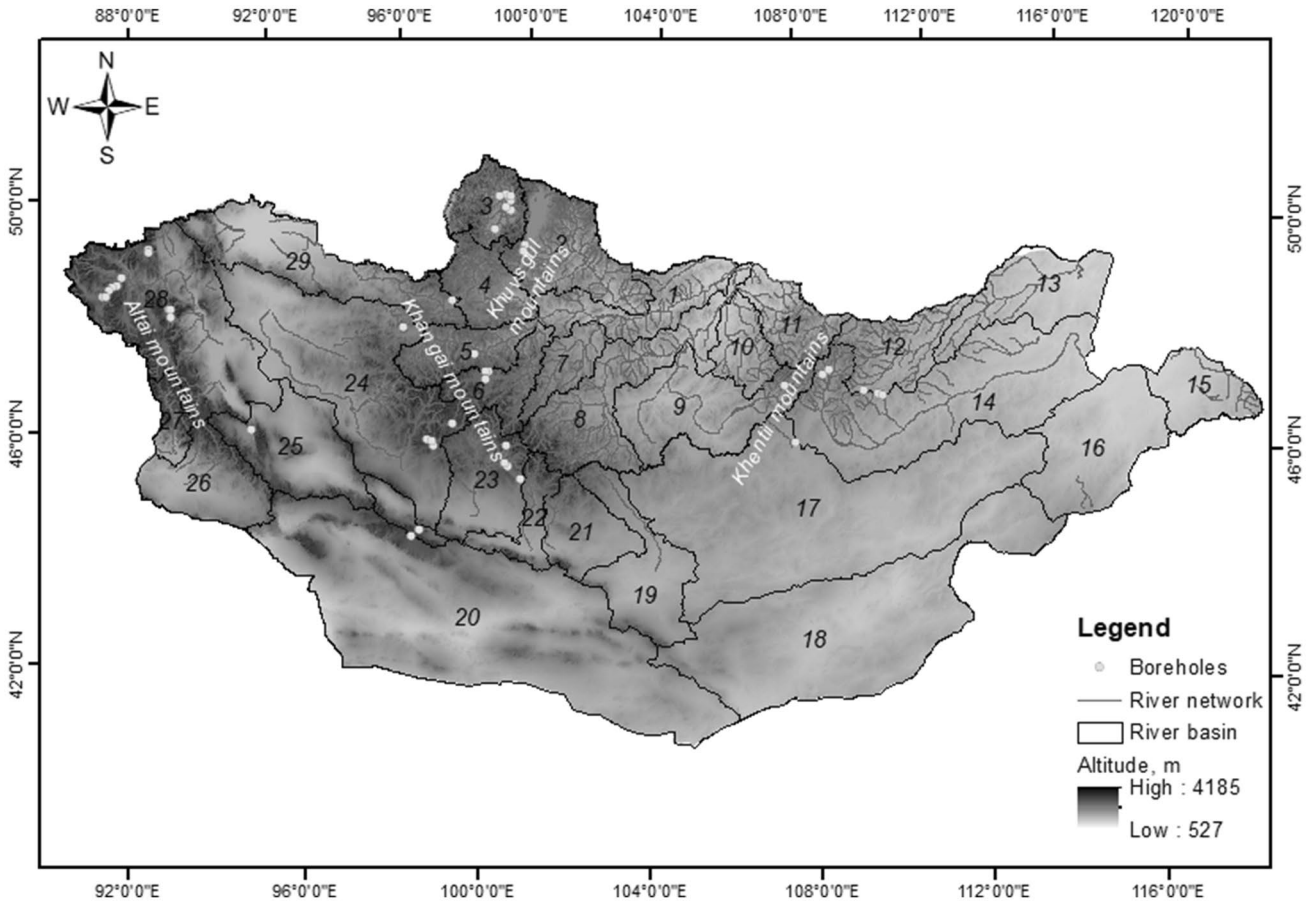

Fig. 1 Location of the observational 34 boreholes in Mongolia. Data of ground temperatures and soil characteristics of the 34 boreholes used to the study

the mean annual land surface temperature ranged from − 0.5 to − 4.3 °C for the Khuvsgul mountain range, + 1 to − 3.6 °C for the Khangai mountain range, + 2.9 to − 5.2 °C for the Altai mountain ranges, and 1.7 to − 0.6 °C for the Khentii mountain range. The Active Layer Thickness (ALT) observed at the boreholes was 1.8–7.7 m. Deeper active layers were observed in the boreholes on the Altai mountains with more shallow ALTs occurred in the Khuvsgul mountain range. Next to temperature, the physical properties of the soil were assessed. These properties include thermal conductivity in thaw and freezing states, volumetric heat capacity, and latent heat of fusion. These values were derived from the predominated soil structure based on as clay, sandy clay, fine sand, and gravely sand which were described by boreholes properties (Jambaljav et al. 2013). Latent heat fusion varies 150–700 J/m^3 and volumetric heat capacity of the soils was found to vary between 11,000 and 40,000 J/m^3. The thermal conductivity varied between 1.3 and 2.19 Wm/°C (Tumurbaatar 2004).

MODIS LSTs' reconstruction method

Land surface temperatures were gathered from the Aqua and Terra MODIS data series in the period August 2012 till August 2013, derived from the Reverb echo tool (https://earthdata.nasa.gov). Day- and night-time MOD11A2 (MODIS/Terra Land surface temperature/Emissivity 8-day L3 global 1 km sin grid V006) and MYD11A2 (The MODIS/Aqua Land surface temperature/Emissivity 8-day L3 global 1 km sin grid V006) contain the global 8-day average gridded dataset with a resolution of 0.928 km. There are seven swathes (sub-images) (h23v03, h23v04, h24v03, h24v04, h25v03, h25v04, and h26v04) mosaicked and re-projected for complete coverage of the Mongolian territory using the MODIS Reprojection Tool (MRTool). This means that one pixel has four LSTs values from day- and night-time images of each MOD11A2 and MYD11A2. Overall, 184 (46*4) mosaicked products were used for this study including 4 day and night time. The spatial interpolation performed the

Table 1 Observational boreholes

No	Mountain ranges	Name of boreholes		Long	Lat	Elevation (m)	Land cover	Depth of temperature measurements (m)
1	Khuvsgul	Arsai pingo-1	BH 1	51,35806	99,71667	1588	Steppe	0,1,3,4,6,8,10,15
2		Arsai pingo-2	BH 2	51,42583	99,72556	1549	Steppe	0,1,3,4,6,8,10,15,25,35
3		Dog hole-1	BH 6	51,18389	99,73750	1591	Mixed forest	0,1,2,3,4,6,8,10
4		Dog hole-2	BH 7	51,18361	99,73889	1559	Mixed forest	0,1,2,3
5		Munguushiin sair	BH 20	50,82083	99,35167	1629	Steppe	0,1,3,4,6,8,10,15
6		Sharga river	BH 22	51,45639	99,58000	1562	Mixed forest	0,1,2,3,4,6,8,9
7		Tsagaannuur	BH 26	51,41139	99,42306	1550	Steppe	0,2,10,15
1	Khangai	Bayanbulag-1	BH 3	46,93222	97,98694	2418	Dry steppe	0,2,10,15
2		Bayanbulag-3	BH 4	46,91917	98,12472	2253	Dry steppe	0,1,2,3,4,6,8,10
3		Bayanovoo	BH 5	46,36611	100,4875	1938	Dry steppe	0,1,2,3,4,5,6,8
4		Galuut-1	BH 10	46,56000	100,1328	2100	Shrubland	0,1,2,3,4,6,8,10
5		Galuut-2	BH 11	46,62472	100,0592	2046	Steppe	0,1,2,3,4,6,8,10
6		Galuut-3	BH 12	46,92306	100,0581	2002	Steppe	0,1,1.5,23
7		Gurvanbulag	BH 13	47,26306	98,60111	2433	Shrubland	0,1,2,4,6,8,12,15
8		Numrug	BH 21	48,90944	97,06583	1853	Steppe	0,1,2,3,4,6,8,10
9		Sharga valley	BH 23	48,55469	99,03494	1896	Steppe	0,1,2,3,4,6,8,10
10		Terkh ar	BH 24	48,09722	99,38861	2180	Steppe	0,1,3,4,6,8,10
11		Terkh valley	BH 25	48,25417	99,39561	2077	Steppe	0,1,3,4,5,6,8,12,14,15
1	Altai	Erdene-1	BH 8	45,29639	97,96500	2695	Desert steppe	0,0.5,1,2.3
2		Erdene-2	BH 9	45,18389	97,78333	2415	Dry steppe	0,1,2,3,4,5,6,7.8
3		Hashaat-1	BH 14	48,47583	90,81194	2080	Dry steppe	0,0.5,1,2,3,4,5
4		Hashaat-2	BH 15	48,60083	90,70611	2498	Steppe	0,0.5,1,2,3,4,6,10
5		Hongor ulun	BH 16	48,60056	90,75167	2390	Steppe	0,2,3,4,6,8,10
6		Tsagaannuur-1	BH 27	49,57472	89,84111	2135	Steppe	0,1,2,3,4,6,8,10
7		Tsagaannuur-2	BH 28	49,51722	89,86361	2113	Desert steppe	0,1,2,3,4,6,8,10
8		Tsengel-1	BH 29	48,99889	89,30083	1995	Steppe	0,1,2,4,6,8,10,15
9		Tsengel-2	BH 30	48,83167	89,19205	2240	Steppe	0,1,2,3,4,8,10
10		Tsengel-3	BH 31	48,80167	89,10944	2338	Steppe	0,1,2,3,4,6,8,10
11		Tsengel-4	BH 32	48,73111	89,00583	2500	Steppe	0,1,2,3,4,6,8,9
12		Tsengel-5	BH 33	48,58417	88,91111	2567	Steppe	0,1,2,3,4,6,8,10
13		Tsengel-6	BH 34	48,58444	88,96972	2556	Dry steppe	0,1,2,3,4,6,8,9
1	Khentii	Khentii50	BH 17	47,85750	110,0686	1405	Steppe	0,1,2,3,4,6,8
2		Mungunmorit-1	BH 18	48,26361	108,5111	1450	Mixed forest	0,1,3,4,6,8,10,15
3		Mungunmorit-2	BH 19	48,35500	108,6844	1496	High mountain steppe	0,1,3,4,6,8,12

missing gaps using the neighbour's values for each image. LSTs of the filled images after spatial interpolation unusually low LSTs removed based on the histogram. Quartile of the histogram follows that the lower outlier was defined as 1st quartile − 1.5 × (1st quartile − 3rd quartile). The unit of the values of the images from MODIS LSTs multiplied by scale factor 0.02 is in Kelvin (Wan 2013). Then, it converted to Celsius by subtracting 273.15°K from it. Finally, the reconstructed fully filled MODIS LSTs of day- and night-time Aqua/Terra datasets were analyzed by panel regression. The regression was applied that observed LSTs from the 34 boreholes are independent values and MODIS LSTs, elevation, latitude, longitude, and slope at the 34 borehole locations area chosen by independent values. The regression is formulated below (Baltagi 2005):

$$Y_{i,t} = \alpha + X_{i,t}\beta + u_{i,t},$$

$i = 1, \ldots, T$ and refers to time-series dimension (8-day average and 46 time-series data for the study); $i = 1, \ldots, N$ and it indicated cross-section dimension (by four seasons or groups including autumn, winter, spring summer, or locations); α is the scalar; $u_{i,t}$ is the error.

Applying TTOP and Kudryavtsev model for estimating the thaw depth

To estimate the mean ground temperature at the top of the permafrost, we used the TTOP approach. TTOP is a simplified formulation of the relationship between climate and permafrost. It estimates the mean annual ground temperatures at the top of the permafrost using the sum of the surface temperature days above and below 0 °C and soil conductivity in thaw/freeze states (Riseborough et al. 2008). Since the TTOP model was introduced by Smith and Riseborough (1996), the model has been applied to several regions for parameter development. Coefficient k was estimated between 0.8 and 0.95 based on the predominated soil mechanics of the soil map:

$$T_{\text{Top}} = \frac{\text{TDD} \times k - \text{FDD}}{P}.$$

TDD is the thawing degree days, °C; FDD is the freezing degree days, °C; k is the ratio of thawed and frozen ground thermal conductivity; P is the period (365 days).

The thaw/freeze depths determined using the Kudryavtsev approach are based on a model for estimating the maximum annual thaw depth of the active layers (Kudryavtsev 1974; Riseborough et al. 2008). This model accounts for the effects of snow cover, vegetation, and regional climate. A valuable method for the computation of the active layer thickness and the mean annual ground temperatures proved to be a modified version of this approach (Romanovsky and Marchenko 2009). The main parameters of this model are the ground surface temperatures and the physical characteristics of the soil:

$$Z_{\text{thaw}} = \frac{2\left(A_s - T_z\right)\sqrt{\frac{\lambda TC}{\pi}} + \frac{\left(2A_zCZ_c + Z_cL\right)L\sqrt{\lambda T/\pi C}}{2A_zCZ_c + LZ_c + \left(2A_zCL\right)\sqrt{\lambda T/\pi C}}}{2A_zC + L},$$

where:

$$T_z = \frac{0.5T_s \cdot \left(\lambda_F + \lambda_T\right) + A_s\frac{\lambda_F - \lambda_T}{\pi} \cdot \left[\frac{T_s}{A_s}\arcsin\frac{T_s}{A_s} + \sqrt{1 - \frac{\pi^2}{A_s^2}}\right]}{\lambda^*},$$

$$\lambda^* = \begin{cases} \lambda_F & \text{if numerator} < 0 \\ \lambda_T & \text{if numerator} > 0 \end{cases}$$

$$Z_c = \frac{2\left(A_z - T_z\right)\sqrt{\lambda TC/\pi}}{2A_zC + L},$$

where:

$$A_z = \frac{A_s - T_z}{\ln\left(\frac{A_s + L/2C}{T_z + L/2C}\right)},$$

where Z_{thaw} is the thawing depths, m; A_s is the annual temperature amplitude at soil surface, °C; T_z is the mean annual temperature at the depth of seasonal thaw, °C; λ is the thermal conductivity, W/m °C; T is the period of temperature wave, s; C is the volumetric heat capacity, J/m^3; L is the volumetric latent heat of fusion, J/m^3; λ_T is the thawing thermal conductivity, W/m °C; λ_F is the freezing thermal conductivity, W/m °C.

Evaluation

Two evaluations were used for this study. The first evaluation was by analyzing the panel regression for MODIS LSTs with observed surface temperatures from the 34 boreholes considering topographic features. Its parameterisation was evaluated with R^2 (between, overall, and within). The other evaluation was done by validating the estimated MAGT from TTOP and ALT from Kudryavtsev with the data of the 34 boreholes using root-mean-square error (RMSE):

$$\text{RMSE} = \sqrt{\frac{\sum_{i=1}^{n}\left(T_{m,i} - T_{o,i}\right)^2}{n}}.$$

Here, $T_{m,i}$ are the estimated values and $T_{o,i}$ are the observed values.

Results

MODIS LST reconstruction

In total, 184 LST datasets with 46 time-series from MODIS were used for the study period. Each image has a spatial coverage of 1,098,281 pixels. Except for missing values, the original MODIS data had to be checked by a Quality Control layer which in included in the MODIS datasets. Quality layer provided for checking error pixels due to could contamination or other reasons. Missing values were under 30% for all images (Fig. 2). Day-time images from Aqua and Terra have more missing values than night-time images. Most missing values counted in winter time in period of November–January.

Spatial interpolation was applied to fill the data gaps of all mosaicked and re-projected MODIS maps. Then, panel regression was performed between MODIS LSTs considering topographic features (elevation, slope, latitude, longitude, and vegetation) and observed land surface temperature at the borehole locations. Cross-section data of the panel were created along the seasons (4 seasons), locations (34

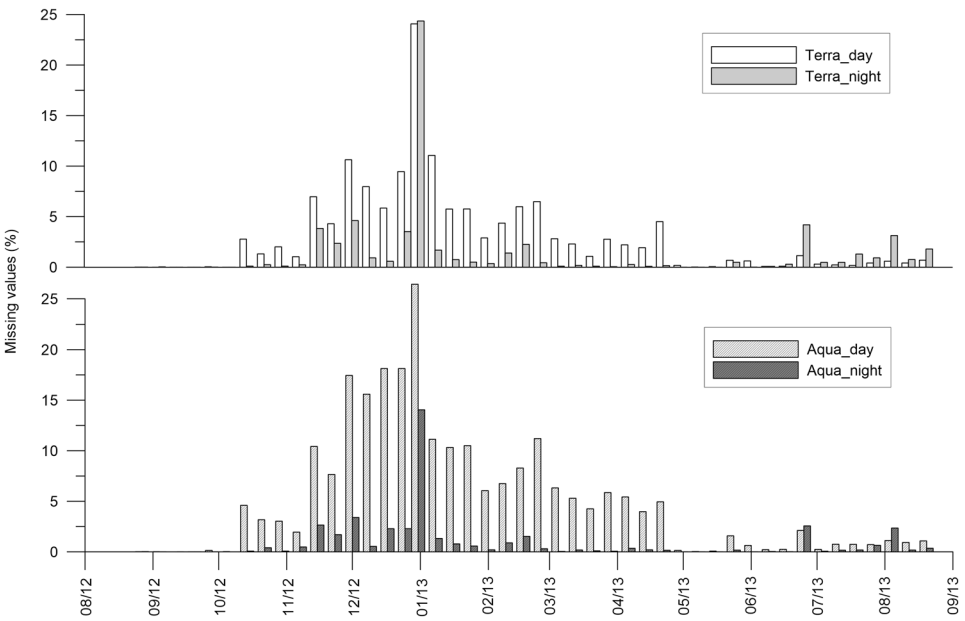

Fig. 2 Missing gaps in Aqua/Terra from MODIS in study period

Table 2 Results of the panel regression analysis

Independent variables	Coefficients	Standard error	*p* value
$Terra_{day}$	0.201	0.023	0.000
$Terra_{night}$	0.345	0.035	0.000
$Aqua_{day}$	0.082	0.022	0.000
$Aqua_{night}$	0.23	0.03	0.000
Elevation	−0.003	0.0005	0.000
Latitude	−0.19	0.09	0.038
Longitude	−0.15	0.03	0.000
Constant	33.3	8.04	0.000

boreholes), and mountains (4 mountain ranges), and time-series data were 46 steps (8 days in a year). The best performance was cross-section data created by the seasons. Then, the parameters of the best panel regression show that observed land surface temperature is significantly (p value < 0.001) related to MODIS LSTs and elevation, latitude, longitude, and slope. Therefore, we selected those parameters with significant related with observed LSTs. The calculated parameters in the best panel regression are given in Table 2.

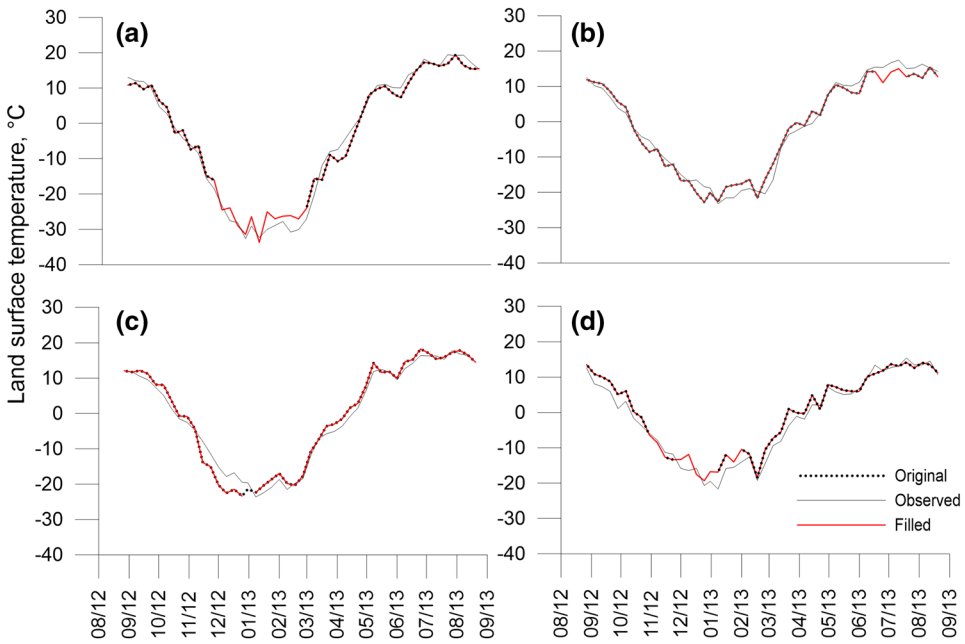

Fig. 3 Estimated land surface temperatures using the filled MODIS LSTs. **a** BH 2 (Arsai-2), **b** BH 4 (Bayanbulag-3), **c** BH 19 (Mungunmorit-1), and **d** BH 34 (Tsengel-3)

The model shows that the land surface temperature can be calculated using the day and night time of Aqua and Terra from MODIS 8-day LSTs considering topographic features. R^2 between observed and modeled LSTs was 0.95. However, seasonally, R were 0.5 in autumn, 0.6 in winter, 0.7 in spring, and 0.8 in spring. Figure 3 illustrates the results from some example boreholes for different mountain ranges.

Spatial distribution of permafrost properties

TDD (thawing degree days) and FDD (freezing degree days) are the main input parameters of the TTOP model. R between observed and estimated TDD and FDD are 0.72 and 0.69, respectively. The average RMSE for observed and modeled TTOP temperature for the boreholes was 0.9 °C. The absolute error between observed and estimated MAGT was under 0.5 °C except for the Tsengel-4, Gurvanbulag, and Tsagaannuur boreholes. The ALT in the permafrost area is 2–3 m in silty soil and 4–5 m in coarse materials in the basins. The average RMSE of observed and estimated ALT was 1.2 m for the boreholes. According to the results of TTOP, overall, 26.3% of the territory of Mongolia is covered by continuous and discontinuous permafrost (Fig. 4).

Table 3 presents the percentages in all river basins of cold permafrost (MAGT < − 2 °C) and warm permafrost (MAGT > − 2 °C) as well as the thickness of the active layer (ALT). The table shows that there is no permafrost in seven river basins. Intersected continuous and discontinuous permafrost distribution are found in 22 basins. According to our results, presented in Table 3, cold permafrost is found more in the Khuvsgul and Altai mountain ranges than in other areas. The table shows that cold permafrost is found in around 30% of the area and warm permafrost in around 40% in the river basins in these mountain ranges. The warm permafrost dominates in the Khentii mountain range. Cold and warm permafrost percentages give good indications of the presence of continuous and discontinuous permafrost conditions in the basin. Cold permafrost occurs in the continuous permafrost zone, while warm permafrost dominates in the discontinuous permafrost zone.

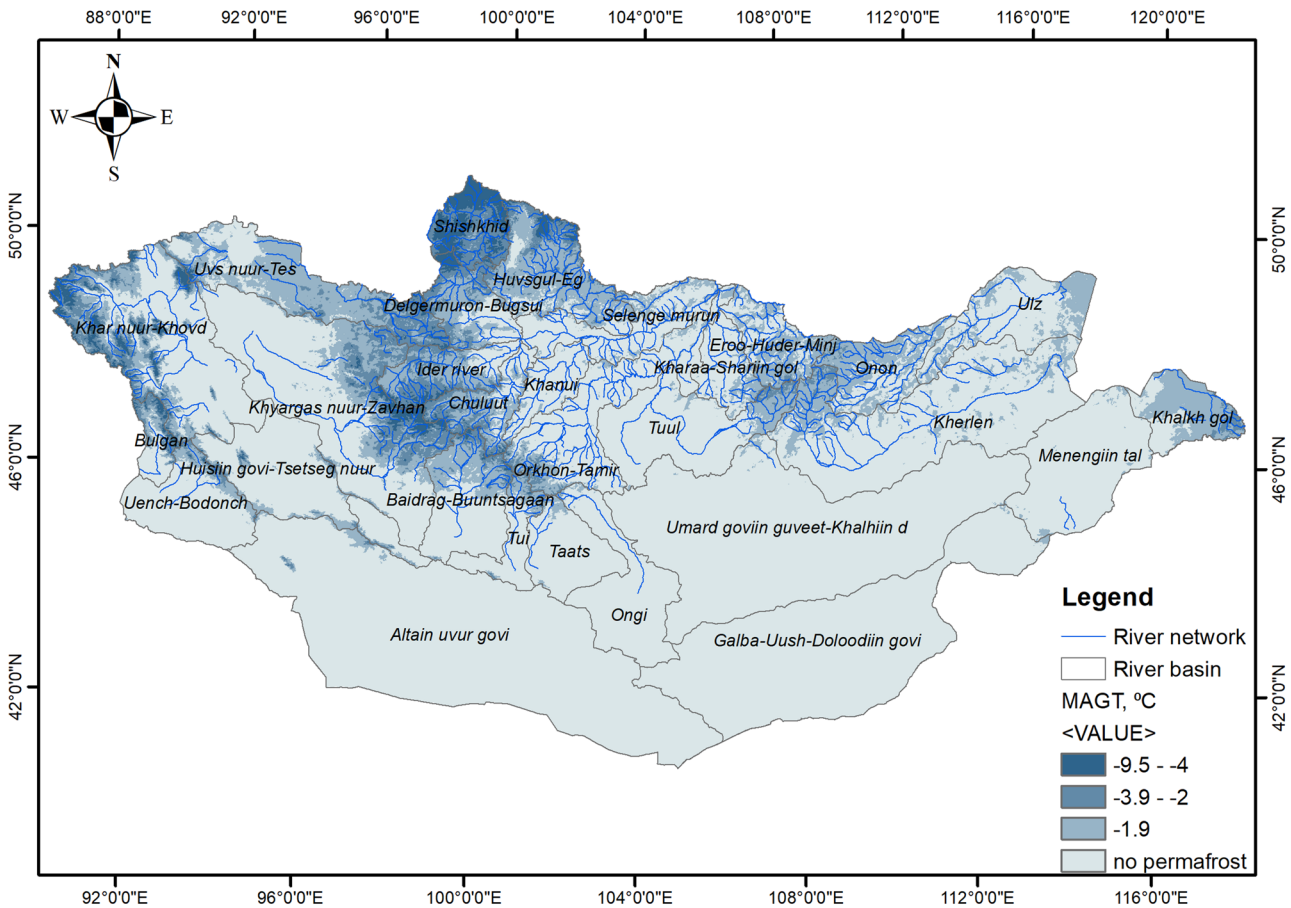

Fig. 4 Result of the MAGT distribution estimated using the TTOP approach

Table 3 Percent of the cold/warm permafrost in the river basins in Mongolia

Mountain ranges	Name of the basins	Area of the basin (km^2)	Percent of the permafrost in the basin (%)			ALT (m)
			Cold permafrost (MAGT < −2 °C)	Warm permafrost (−2 °C < MAGT < 0 °C)	MAGT (°C)	
Altai	Khar nuur-Khovd	87,767	22.6	19.5	−2.5	0.9–4.6
	Uench-Bodonch	34,037	4.7	11.1	−1.7	0.8–3.5
	Uvs nuur-Tes	53,510	21.7	56.2	−1.4	2.7–4.9
	Khyargas nuur-Zavkhan	120,707	17.6	17.6	−1.2	0.9–4.1
Khangai	Baidrag-Buuntsagaan	35,153	30.1	10.1	−0.5	0.9–3.2
	Bulgan	10,022	34.8	20.2	−0.6	1.2–3.9
	Chuluut	19,813	30.0	41.4	−1.4	1.5–4.0
	Khanui	15,5496	0.5	7.1	−0.2	2.2–3.2
	Ider	22,757	39.8	40.6	−1.6	1.9–4.2
	Ongi	39,202	0.0	0.0	–	0
	Orkhon	52,753	3.8	13.3	−1.6	2.1–3.4
	Selenge	30,983	0.6	21.7	−0.7	1.4–3.6
	Taats	25,092	0.2	4.9	−0.6	0.8–3.3
	Tui	15,529	17.6	6.2	−0.9	0.9–3.3
Khentii	Eruu-Huder-Minj	21,986	3.1	61.1	−1.9	2.4–3.7
	Khalkh	23,443	0.0	0.0	−0.5	0
	Kharaa-Shariin gol	17,463	0.7	21.8	−0.8	2.3–3.6
	Kherlen	106,487	1.6	16.1	−0.9	1.3–3.5
	Onon	27,870	2.8	64.6	−1.2	2.6–3.6
	Tuul	49,416	3.7	11.6	−1.1	1.3–3.6
	Ulz	37,462	0.0	0.0	–	0
Khuvsgul	Delgermurun-Bugsui	23,018	35.8	37.9	−2.3	2.6–5.2
	Khuvsgul–Eg	41,321	23.7	61.4	−1.7	1.5–4.4
	Shishkhid	20,096	46.0	51.7	−4.1	1.7–7.2
Govi	Altain uvur govi	218,250	0.0	0.0	–	0
	GalbaUush-Doloodiin govi	14,0416	0.0	0.0	–	0
	Huisiin govi-Tsetseg nuur	42,460	2.6	10.1	−0.9	0.9–3.2
	Menengiin tal	53,372	0.0	0.0	–	0
	Umard goviin guveet-Khalkhiin dundad tal	178,182	0.0	0.0	–	0

Discussion

Ground surface temperature is one of the crucial factors for permafrost research. To estimate the permafrost distribution in a basin, ALT and MAGT were estimated successfully using the reconstructed ground surface temperatures. The results confirm the first hypothesis of the study that topographic features are independent factors for surface temperatures. Latitude, longitude, elevation, and slopes were improved in the model performance for reconstructing the MODIS LSTs in this study. Multi-regression methods were used in the number of studies which conducted day- and night-time Terra/Aqua MODIS LSTs regressed with observed surface temperatures (Zou et al. 2017) and some of them considered with topographic features (Metz et al. 2017). It is dependent on regional and/or local climate and terrain characteristics. Using the panel regression method gives many model tests building different cross-sectional data compared with the traditional regression.

As defined negative MAGT allows the permafrost occurrence by the TTOP approach, the results show that river basins in the Khuvsgul mountain range are covered by the permafrost for approximately 70–97% of their areas. The permafrost coverage is 15–60% in the Khentii mountain, 15–70% in the Altai mountain, and 10–30% in the Khangai mountain range (Table 3). Most of the rivers originate from mountains of those ranges underlain by the permafrost. Similar observation concluded by Iijima et al. (2012) showed that the areas of permafrost in Mongolia occur in the overlap with a major source of the surface water. Knowing the distribution and type of permafrost at basin level is important for assessing the impact of climate change on surface water

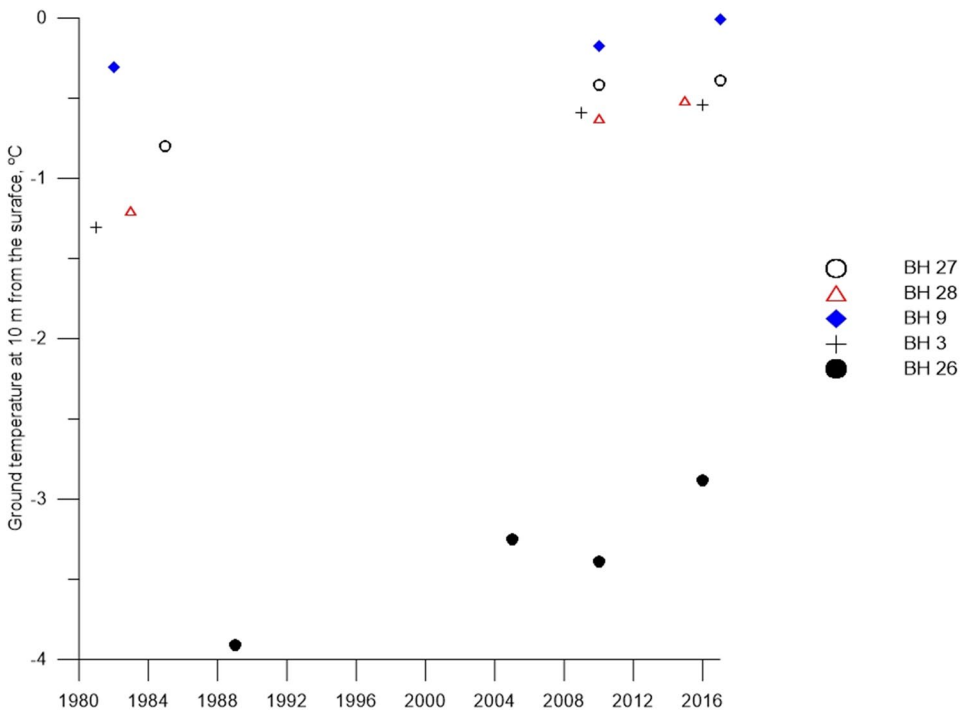

Fig. 5 Ground temperature measurements at 10 m below surface for some boreholes in Mongolia for the period 1980 to 2016. In the graph, BH 3 is a borehole in the Khuvsgul mountain range. BH9, BH 27, and BH 28 are located in the Altai mountain range. BH 26 is located in the Khangai mountain range

system in the permafrost region. Several studies (Sharkhuu 2003; Kynický et al. 2009) reported that the permafrost is degrading in Mongolia due to climate change. A few boreholes with data since 1980 show that ground temperatures at 10 m below surface increased at different rates between 0.4 and 1 °C (Fig. 5). Degrading permafrost conditions due to climate change will affect the surface water system depending on the distribution and type of the permafrost. In other words, in an area that includes permafrost and non-permafrost, the percentage of permafrost drives the hydrological characteristics (Wang et al. 2018).

In context of the warm and cold permafrost, the results did not appear to support the second hypothesis. In contrast to the second hypothesis, the warm permafrost was predominated in the river basins of Mongolia. It means that the MAGT is from 0 to − 2 °C in the discontinuous and sporadic extents. Our data based on observational 34 boreholes over a year show that the negative MAGT or permafrost occurrence is strongly related with the ground surface temperatures. Cold climate or low ground surface temperature is the main factor for the spatial distribution of permafrost in Mongolia.

Not only climate but also terrain factors affect the spatial distribution of the permafrost. Many studies concluded that topographic depression (Ishikawa et al. 2018) or other factors such as elevation, topographic wetness, solar radiation, vegetation, and snow cover (Etzelmuller et al. 2006; Goncharova et al. 2019) are crucial to the permafrost distribution. The elevation and latitude are another certain factors for the permafrost occurrence in Mongolia (Kynický et al. 2009), especially it is obviously shown for the boreholes in the Altai mountain range. It is also proven that cold permafrost is predominantly distributed in a few river basins with the highest elevation of the Khuvsgul, Altai, and Khangai mountain ranges (Table 3). As another terrain factor, different vegetation covers coincide with extent of permafrost as continuous, discontinuous, and sporadic, especially forest areas overlap with permafrost occurrence (Tsogtbaatar 2004). General pattern of the MAGT map is overlain with forest areas, as well. Forest can lead to promote permafrost existence by maintaining low soil temperature and by reducing soil moisture (Runyan and D'Odorico 2012). Specially, north facing slopes occupy forest due to low percentage of exposure to solar radiation. Moreover, moss cover, dense grass, and tall shrubs reduce surface temperature in summer time, and they are other crucial factors for the permafrost distribution as continuous and discontinuous zones (Sharkhuu and Anarmaa 2012). Those surface factors are contributory factors for the permafrost distribution and especially warm permafrost controlled by ecosystem (Ishikawa et al. 2018).

Conclusions

To determine the spatial distribution of the permafrost of Mongolia, we used reconstructed MODIS LTSs to estimate MAGT and ALT. Different methods were applied in to a diverse range of systems to fill the gaps caused by probability of cloud contamination of MODIS LSTs (Malamiri et al. 2018; Metz et al. 2017). In our study, a panel regression

approach was found to work well for reconstruction of the MODIS LSTs of Mongolia. Earlier studies (Mustrer et al. 2015; Zou et al. 2017; Wu et al. 2018a, b) agreed that the reconstructed MODIS LSTs provide a reasonable input for permafrost studies.

In this study, we produced a new map, showing that the spatial distribution of different types of permafrost covers about 26.3% over Mongolia. The map is based on the MAGT and ALT values that were derived from merging temperature time-series and soil characteristics in 34 observational boreholes across Mongolia with 8-day LSTs of MODIS using the TTOP approach and the Kudryavtsev model. The time-series observations covered 1 year, starting in August 2012. Statistically reconstructed MODIS 8-day LSTs have been used for modelling the general distribution of the MAGT and ALT in Mongolia. The distribution shows major differences in cold and warm permafrost over the country. The results were validated using a limited subset of the borehole data.

Intersecting river basins to the MAGT, the cold permafrost is found abundantly in the Khuvsgul and Altai mountain ranges and in some rivers in Khangai mountain range. The warm permafrost is dominated in the Khentii mountain range. In general, the ALT in the permafrost area is 2–3 m in clay soil and 4–5 m in gravelly sand materials in the basins. The average MAGT and ALT for the permafrost regions is − 1.6 °C and 3.1 m, respectively. The highest distribution of cold and warm permafrost is found in river basins of northern Mongolia, an area that has a high density of river network and provides a major part of the surface water resources of the country.

References

Baltagi BH (2005) Econometric analysis of panel data, 3rd edn. Wiley, New York

Etzelmuller B, Heggem ESF, Sharkhuu N, Frauenfelder R, Kaab A, Goulden C (2006) Mountain permafrost distribution modelling using a multi-criteria approach in the Hovsgol area, Northern Mongolia. Permafr Periglac Process 17:91–104. https://doi.org/10.1002/ppp554

Gonrachova OYu, Matyshak GV, Epstein HE, Sefilian AR, Bobrik AA (2019) Influence of snow cover on soil temperatures: Meso-and micro-scale topographic effects (a case study from the northern West Siberia discontinuous permafrost zone). CATENA. https://doi.org/10.1016/j.catena.2019.104224

Hachem S, Allard M, Duguay C (2009) Using the MODIS land surface temperature product for mapping permafrost: an application to northern Quebec and Labrador, Canada. Permafr Periglac Process. https://doi.org/10.1002/ppp672

Hall DK, Box JE, Casey KE, Hook JS, Shuman CA, Steffen K (2008) Comparison of satellite derived and mustrerin situ observations of ice and snow surface tempertaures over Greenland. Remote Sens Environ. https://doi.org/10.10106/j.re.2008.05.007

Huang R, Zhang Ch, Huang J, Zhu D, Wang L, Liu J (2015) Mapping of daily mean air tempertaure in agricultural regions using daytime and nighttime land surface temperatures derived from Terra and Aqua Modis data. Remote Sens 7:8728–8756. https://doi.org/10.3390/rs70708728

Iijima Yo, Ishikawa M, Ya Jambaljav (2012) Hydrological cycle in relation to permafrost environment in forest-grassland ecotone in Mongolia. J Japan Assoc Hydrol Sci 42(3):119 (**Abstract in English**)

Ishikawa M, Jambaljav Ya, Dashtseren A, Sharkhuu N, Davaa G, Yo I, Baatarbileg N, Yoshikawa K (2018) Thermal states, responsiveness and degredation of marginal permafrost in Mongolia. Permafr Periglac Process 29:271–282. https://doi.org/10.1002/ppp.1990

Jambaljav Ya et al (2013) Report on permafrost monitoring of Mongolia. Permafrost sector, Institute of Geography. Mongolian Academy of Sciences. No:201300095 **(in Mongolian)**

Jambaljav Ya, Gansukh Ya, Saruulzaya A, Sharkhuu, N (2017) Permafrost change in Mongolia. In: Nyamdavaa A, Avid B (eds) Environment of Mongolia, vol I. Admon Printing, Ulaanbaatar, pp 191–254 **(in Mongolian)**

Kynický J, Brtnický M, Vavříček D, Bartošová R, Majigsuren U (2009) Permafrost and climatic change in Mongolia. Sustainable Development and Bioclimate 1.vyd. Stara Lesna

Kudryavtsev VA (1974) Fundamentals in permafrost forecasting in geotechnical studies. University of Moscow, Moscow **(in Russian)**

Langer M, Westermann S, Heikenfeld M, Dorn W, Boike J (2013) Satellite-based modeling of permafrost temperatures in a tundra lowland landscape. Remote Sens Environ. https://doi.org/10.1016/j.rse.2013.03.11

Malamiri HR, Rousta I, Olafsson H, Zare H, Zhang H (2018) Atmosphere. https://doi.org/10.3390/atmos9090334

Metz M, Andreo V, Neteler M (2017) A newly fully gap-free time series of land surface tempertaure from MODIS LST data. Remote Sens 9(12):1333. https://doi.org/10.3390/rs9121333

Mustrer S, Langer M, Abnizova A, Young KL, Boike J (2015) Spatio-temporal sensitivity of MODIS land surface tempertuares anomalies indicates high potential for large scale land cover change detection in Arctic permafrost landscapes. Remote Sens Environ. https://doi.org/10.1016/j.rse.2015.06.017

Neteler M (2010) Estimating daily land surface temperatures in mountainous environments by reconstructed MODIS LST data. Remote Sens 2:333–351. https://doi.org/10.3390/rs1020333

Niu F, Yin G, Luo J, Lin Zh, Liu M (2018) Permafrost distribution along the Qinghai-Tibet enginerring corridor, China using High-resolution statistical mapping and modeling integrated with `remote sensing and GIS. Remote Sens 10(2):215. https://doi.org/10.3390/rs10020215

Pede T, Mountrakis G (2018) An empirical comparison of interpolation methods for MODIS 8-day land surface temperature composites across the conterminous United States. J Photogramm Remote Sens. https://doi.org/10.1016/j.isprsjprs.2018.06.003

Qi J, Niu Sh, Zhao Y, Liang M, Ding Y (2017) Response of vegetation growth to climatic factors in Shule river basin in Northwest China: A panel analysis. Sustainability 9(3):368. https://doi.org/10.3390/su9030368

Riseborough D, Nikolay S, Etzelmuller B, Gruver S, Marchneko S (2008) Recent advances in permafrost modeling. Permafr Periglac Process. 10.1002/ppp.615, p137-156

Romanovsky VE, Marchenko S (2009) The GIPL permafrost dynamics model. University of Alaska, Fairbanks

Romanovsky VE, Smith SL, Christiansen HH (2010) Permafrost thermal state in the polar Northern Hemisphere during the international polar year 2007–2009: a synthesis. Permafr Periglac Process. https://doi.org/10.1002/ppp.689

Runyan CW, D'Odorico P (2012) Ecohydrological feedbacks between permafrost and vegetation dynamics. Adv Water Resour. https://doi.org/10.1016/j.advwatres.2012.07.016

Sharkhuu N (2003) Recent changes in the permafrost of Mongolia. In: Proceeding of the 8th international conference on permafrost, pp 1029–1034

Sharkhuu N, Anarmaa Sh (2012) Effects of climate warming and vegetation cover on permafrost of Mongolia. In: Werger M, van Staalduinen M (eds) Eurasian Steppes. Ecological problems and livelihoods in a changing world. Plant and vegetation, vol 6. Springer, Dordrecht. https://doi.org/10.1007/978-94-007-3886-70_17

Shi K, Chen Y, Yu B, Xu T, Chen Z, Liu R, Li L, Wu J (2016) Modeling spatiotemporal CO2 (carbon dioxide) emission dynamics in China from DMSP-OLS nighttime stable light data using panel data analysis. Appl Energy 168(C):523–533. https://doi.org/10.1016/j.apenergy.2015.11.055

Smith MW, Riseborough DW (1996) Permafrost monitoring and detection of climate change. Permafr Periglac Process 7(4):301–309. https://doi.org/10.1002/(SICI)1099-1530(199610)7:4<301:AID-PPP231>3.0.CO;2-R

Smith SL, Romanovsky VE, Lewkowicz AG, Burn CR, Allard M, Clow GD, Yoshikawa K, Troop J (2010) Thermal state of permafrost in North America: a contribution to the international polar year. Permafr Pergilac Process. https://doi.org/10.1002/ppp.690

Tsogtbaatar J (2004) Deforestation and reforestation needs in Mongolia. For Ecol Manage. https://doi.org/10.1016/j.foreco.2004.06.011

Tumurbaatar D (2004) Seasonally frozen ground and permafrost in Mongolia. Urlakh Erdem Press, Ulaanbaatar

Wan Zh (2013) Collection-6 MODIS land surface temperature products users' guide. ICESS, Santa Barbara, CA

Wang X, Chen R, Liu G, Han Ch, Yang Y, Song Y, Liu J, Liu Zh, Liu X, Guo Sh, Wang L, Zheng Q (2018) Responcse of low flows under climate warmng in high-altitude permafrost regions in wester China. Hydrol Process. https://doi.org/10.1002/hyp.13311

Wu Q, Zhang T, Liu Y (2010) Permafrost temperatures and thickness on the Qinghai-Tibet Plateau. Global Planet Change. https://doi.org/10.1016/j.gloplacha.2010.03.001

Wu P, Liang S, Wang XS, Feng Y, McKenzie M (2018a) Climate-induced hydrologic change in the source region of the Yellow river: a new assessment including varying permafrost. Hydrol Earth Syst Sci Discuss. https://doi.org/10.5194/hess-2017-744

Wu X, Nan Zh, Zhao Sh, Zhao L, Cheng G (2018b) Spatial modeling of permafrost distribution and properties on the Qinghai-Tibet Plateau. Permafr Peroglac Process. https://doi.org/10.1002/ppp.1971

Xu Y, Shen Y, Wu Z (2013) Spatial and temporal variations of land surface tempertaure over the Tibean Plateau based on harmonic analysis. Mt Res Dev 33(1):85–94. https://doi.org/10.1659/MRD-journal-d-12-00090.1

Yu D (2015) Exploring spatiotemporally varying regressed relationships: the geographically weighted panel regression analysis. In: International archives of the photogrammetry, remote sensing and spatial information sciences—ISPRS archives, vol 38, pp 134–139

Zhao L, Wu Q, Marchenko SS, Sharkhuu N (2010) Themal state permafrost and active layer in Central Asia during International polar year. Permafr Periglac Process 21:198–207. https://doi.org/10.1002/ppp.668

Zou D, Zhao L, Sheng Y, Chen J, Guojie Hu et al (2017) A new map of permafrost distribution on the Tibetan Plateau. Cryosphere 11(6):2527–2542. https://doi.org/10.5194/tc-11-2527-2017

Publisher's Note Springer Nature remains neutral with regard to jurisdictional claims in published maps and institutional affiliations.